

# Preferred orientation of $\text{Si}_3\text{N}_4$ ceramics by slip casting in a high magnetic field

Shuqin Li<sup>\*</sup>, Kensuke Sassa, Shigeo Asai

*Department of Materials Processing Engineering, Graduate School of Engineering,  
Nagoya University, Furo-cho, Chikusa Nagoya 464-8603, Japan*

Received 12 January 2004; received in revised form 13 February 2005; accepted 24 May 2005

Available online 18 August 2005

## Abstract

Preferred orientation of  $\text{Si}_3\text{N}_4$  ceramics by slip casting in a high magnetic field was obtained. Although the magnetic susceptibility of non-magnetic  $\text{Si}_3\text{N}_4$  ceramics is very small, it is possible to control the crystal orientation of  $\text{Si}_3\text{N}_4$  using a high magnetic field. The orientation of  $\text{Si}_3\text{N}_4$  ceramics was studied by X-ray diffraction and the orientation degree was calculated. The results indicated that  $\beta\text{-Si}_3\text{N}_4$  phase possessed  $a$ ,  $b$ -axis orientation parallel to the magnetic field and  $c$ -axis orientation perpendicular to the magnetic field. SEM micrographs of polished and plasma etched specimens showed  $a$ ,  $b$  planes of  $\beta\text{-Si}_3\text{N}_4$  grains aligned in the side2 surfaces.

© 2005 Elsevier Ltd and Techna Group S.r.l. All rights reserved.

**Keywords:** A. Slip casting; D. Silicon nitride; Preferred orientation; High magnetic field

## 1. Introduction

Silicon nitride is one of the most promising ceramic materials for use in gas turbine engines and other high-temperature structural applications due to its high-temperature strength, thermal shock resistance, chemical stability, and excellent creep resistance and good resistance to oxidation. However, the low toughness still hampers  $\text{Si}_3\text{N}_4$  wide potential application and has to be improved.

Recently, the magnetic field has been recognized as a tool to control microstructure and performance of materials [1]. Moreover, the controlled development of oriented microstructures in ceramics is one way of effectively improving their properties [2,3]. So in this study, the control of the crystal orientation of the  $\text{Si}_3\text{N}_4$  has been studied under the high magnetic field generated by a superconducting magnet.

## 2. Experiment procedure

Commercially available  $\alpha\text{-Si}_3\text{N}_4$  powder (Mitsuwa Pure Chemicals Co. Ltd., Japan, mean diameter:  $0.7\text{ }\mu\text{m}$ ) was used together with a mixture of 8 wt.%  $\text{Y}_2\text{O}_3$  and 4 wt.%  $\text{Al}_2\text{O}_3$  as the sintering aid. The fabrication process of  $\text{Si}_3\text{N}_4$  ceramics by slip casting in the magnetic field is shown in Fig. 1.

The dispersion of powder into an individual particle is necessary for effective utilization of a magnetic field, because the agglomerated particles in a suspension prevent each particle motion from rotating under the application of a magnetic field [4]. In this study, the slip casting process was used. During slip casting, the repulsive surface force can avoid agglomerates and it results very effective in developing consolidated fine particles.

The  $\alpha\text{-Si}_3\text{N}_4$ , and  $\text{Y}_2\text{O}_3$  and  $\text{Al}_2\text{O}_3$  batch was milled in distilled water followed by drying, sieving and calcinations at  $600\text{ }^\circ\text{C}$  [5], then the powder was dispersed in distilled water with tetramethylammonium hydroxide (TMAH) as deflocculant and at the same time, NaOH solution was used to adjust the PH value at 11.5 to ensure dispersion by electrosteric repulsion between the particles [6]. After the suspension with 65 wt.% solids was dispersed by an

<sup>\*</sup> Corresponding author. Tel.: +81 52 789 3248; fax: +81 52 789 3247.  
E-mail address: lishuqin97@hotmail.com (S. Li).

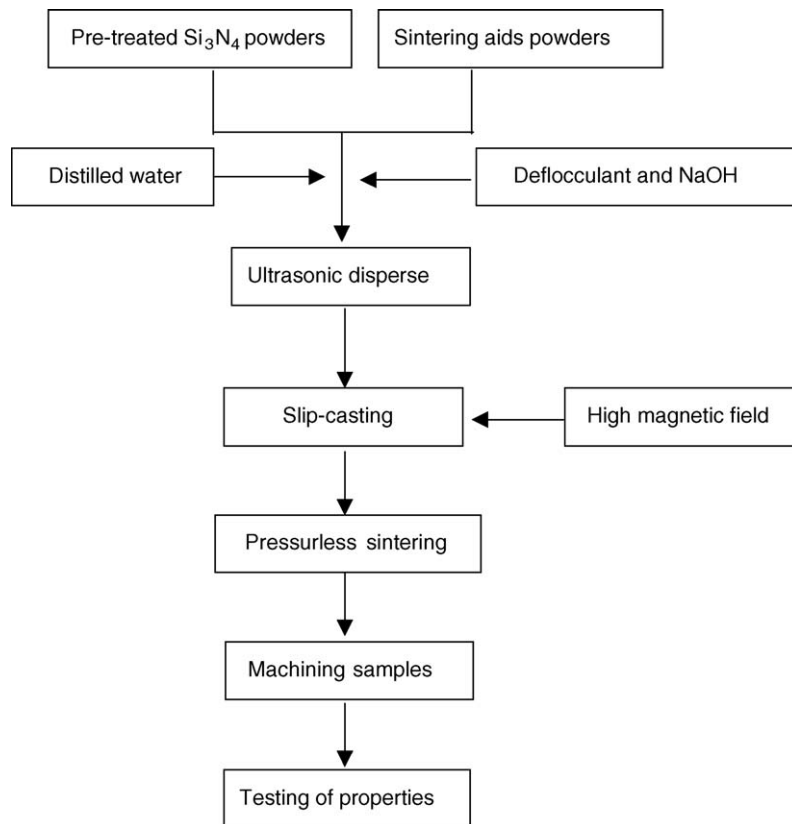


Fig. 1. Flow chart for fabrication of  $\text{Si}_3\text{N}_4$  ceramics.

ultrasonic wave for 30 min, it was poured into a gypsum mold, and left to consolidate. A high magnetic field of 10 T was applied to the suspension during the slip casting at room temperature. The direction of the magnetic field was perpendicular to the direction of the gravity. Figs. 2 and 3 show the schematic view of the experimental apparatus and the definition of the specimen surfaces. In order to compare the effect of the slip casting process on the texture, a green sample was also prepared without the magnetic field. After drying, the green samples were embedded in 50 wt.%

$\text{Si}_3\text{N}_4 + 40 \text{ wt.}\% \text{ BN} + 10 \text{ wt.}\% \text{ MgO}$  powder bed in a graphite crucible, sintered to  $1800^\circ\text{C}$  for 1.5 h in  $\text{N}_2$  atmosphere without the magnetic field. And subsequently cut in top and side surfaces to the imposed magnetic field. Orientation indexes on these planes were calculated from the X-ray diffraction patterns. Meanwhile, microstructure analysis of the surfaces of the samples, which were polished with diamond pastes and etched with molten NaOH at  $400^\circ\text{C}$  for 1.5 min, was carried out by scanning electron microscopy (SEM).

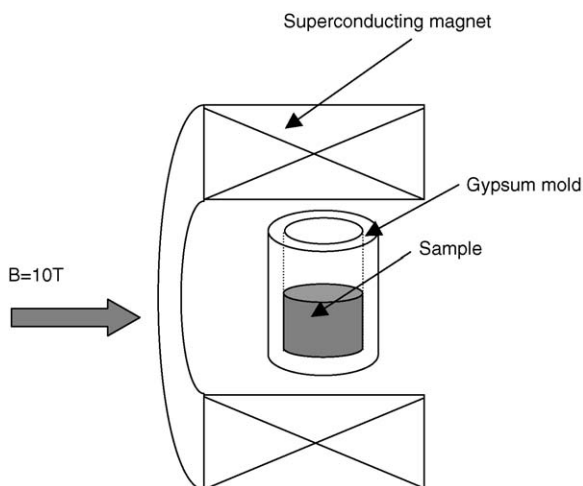


Fig. 2. Schematic view of experimental apparatus.

### 3. Results and discussion

Fig. 4(a and b) shows the XRD profiles of the sample prepared by the slip casting without a magnetic field. It can be seen that the peaks intensities in top and side surfaces are different. However, the orientation is not obvious. Fig. 4(c–e)

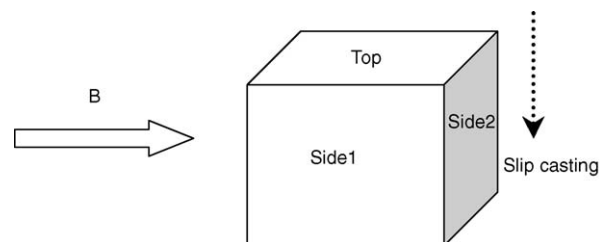


Fig. 3. The definition of the specimen surfaces.

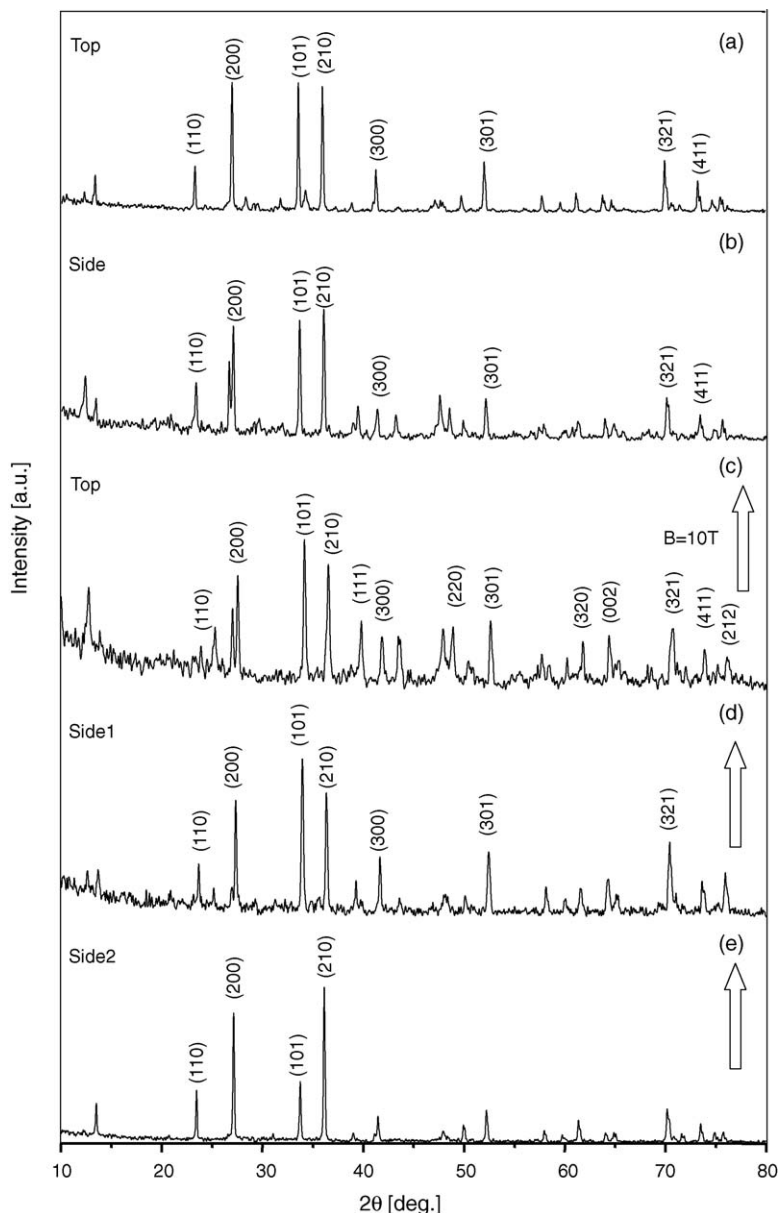


Fig. 4. X-ray diffraction patterns of  $\beta$ - $\text{Si}_3\text{N}_4$  sample obtained from the slip casting method without and with a magnetic field.

illustrate the XRD profiles of the sample prepared by slip casting under a magnetic field of 10 T and followed by sintering at 1800 °C for 1.5 h without the magnetic field. No peaks are visible for  $\alpha$ - $\text{Si}_3\text{N}_4$ , so it can be confirmed that  $\alpha$ - $\text{Si}_3\text{N}_4$  fully transforms to  $\beta$ - $\text{Si}_3\text{N}_4$  after sintering. Moreover, it can be seen that the magnetic field can affect crystal orientation. In the top and side1 surface parallel to the magnetic field in Fig. 4(c and d), the intensity of the (1 0 1) peak is very large and the intensity of (2 1 0) and (2 0 0) peaks is relatively small compared to the peaks in the side2 surface of the sample which is perpendicular to the magnetic field direction (in Fig. 4(e)). Above results indicate that  $a$ ,  $b$ -axis orientation to the magnetic field direction appears. XRD data of  $\beta$ - $\text{Si}_3\text{N}_4$  phases on the top, side1 and side2 surfaces are listed in Table 1.

The intensity of each  $\{hkl\}$  peak  $\text{Si}_3\text{N}_4$  phase,  $I_{hkl}$ , is given by [7]:

$$I_{hkl} = \left( \frac{I_0 A_{hkl} \lambda^3}{32\pi r} \right) \left[ \left( \frac{\mu_0}{4\pi} \right) \frac{e^4}{m^2} \right] \frac{1}{v^2} \times \left[ F^2 P \left( \frac{1 + \cos^2 \theta}{\sin^2 \theta \cos \theta} \right) \right] \frac{e^{-2M}}{2\mu} \quad (1)$$

where  $I_0$  is the incident beam intensity,  $A_{hkl}$  the incident beam cross-sectional area,  $\lambda$  the incident beam wavelength,  $r$  the radius of the diffractometer circle,  $\mu_0$  a constant with a value of  $4\pi \times 10^{-7} \text{ m kg c}^{-2}$ ,  $e$  the electron charge,  $m$  the electron mass,  $v$  the unit-cell volume,  $F$  the structure factor,  $P$  the multiplicity factor, and  $\mu$  the linear absorption

Table 1

The XRD data of  $\beta$ - $\text{Si}_3\text{N}_4$  phase in the sintered sample

$hkl$	$D$ (Å)	$2\theta$ (°)	$I/I_0$ in JCPDS card (%)	$I/I_0$ (%) (top)	$I/I_0$ (%) (side1)	$I/I_0$ (%) (side2)
1 0 0	6.5826	13.440	34	21	22	17
1 1 0	3.8017	23.380	35	32	25	5
2 0 0	3.2924	27.060	100	71	70	75
1 0 1	2.6620	33.640	99	100	100	37
2 1 0	2.4887	36.060	93	89	78	100
1 1 1	2.3121	38.920	9	26	37	6
3 0 0	2.1964	41.060	10	17	28	21
2 2 0	1.9020	47.780	8	18	27	8
3 1 0	1.8267	49.880	12	16	20	14
3 0 1	1.7528	52.140	37	13	31	18
2 2 1	1.5918	57.880	12	23	23	10
3 1 1	1.5476	59.700	6	14	25	7
3 2 0	1.5110	61.300	15	12	21	25
0 0 2	1.4534	63.940	15	22	41	9
4 1 0	1.4368	64.840	8	15	20	20
3 2 1	1.3413	70.100	39	38	61	22
4 1 1	1.2892	73.380	18	22	33	8
2 1 2	1.2679	74.820	16	37	33	6

coefficient for the mixture.  $I_{hkl}$  the intensity of  $\{hkl\}$  peak of  $\text{Si}_3\text{N}_4$  phase in the material.

In order to calculate the degree of orientation in the material, the relative orientation density,  $J_{hkl}$ , is given by [8]:

$$J_{hkl} = \frac{A_{hkl}/A_{\text{total}}}{A_{hkl}^0/A_{\text{total}}^0} \quad (2)$$

where,  $A_{hkl}$  and  $A_{\text{total}}$  are the incident beam cross-sectional area of  $\{hkl\}$  plane and total incident beam cross-sectional area in the sample, and  $A_{hkl}^0$  and  $A_{\text{total}}^0$  are for the material without orientation. The value of  $J_{hkl}$  can reflect the orientation degree of different crystal planes. When  $J_{hkl} > 1$ ,  $\{hkl\}$  planes prefer to parallel to sample surface; when  $J_{hkl} = 1$ ,  $\{hkl\}$  planes distribute randomly; and when  $J_{hkl} < 1$ ,  $\{hkl\}$  planes take up an alternative orientation. A quantitative measurement to calculate the  $J_{hkl}$  value of each plane is presented:

$$J_{hkl} = \frac{I_{hkl}/\sum I_{hkl}}{I_{hkl}^0/\sum I_{hkl}^0} \quad (3)$$

where,  $I_{hkl}$  and  $I_{hkl}^0$  are the intensities of the  $\{hkl\}$  peaks in the samples with and without orientation.

In order to show the preferred orientation degree of  $\beta$ - $\text{Si}_3\text{N}_4$  phase elongated grains, the  $J_{101}/J_{200}$  was used to indicate the orientation of the  $\text{Si}_3\text{N}_4$  phases. The formula is:

$$F = \frac{J_{101}}{J_{200}} = \frac{I_{101}/I_{101}^0}{I_{200}/I_{200}^0} \quad (4)$$

If  $F = 1$ , the rod-like grains are scattered randomly. The larger the  $F$  value, the more strongly the grains possess  $c$ -axis orientation; the smaller the  $F$  value, the more strongly the grains possess  $a, b$ -axis orientation. From Table 1, it can be calculated that  $F$  value of the sample in the topside is 1.43, in side1, 1.44 and in side2, 0.50. From this result, it can be seen that the sample shows  $c$ -axis orientation in the top and side1 surface, and  $a, b$ -axis orientation in the side2 surface. The anisotropic susceptibility of  $\alpha$ - $\text{Si}_3\text{N}_4$  with a hexagonal asymmetric unit cell can produce the energy of anisotropy in a magnetic field. The energy of anisotropy,  $\Delta E$ , associated with the crystals is expressed by the following

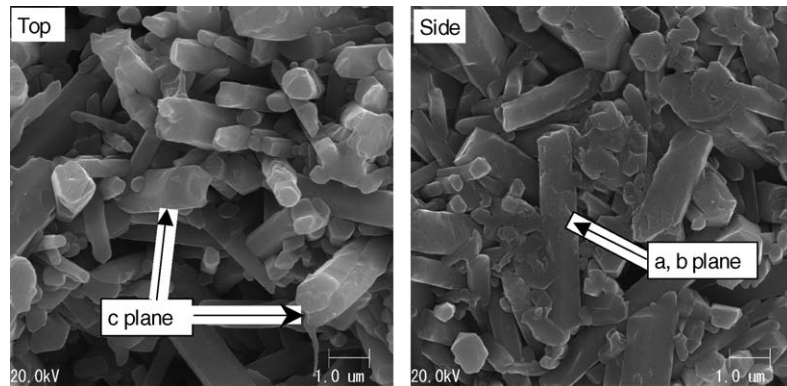


Fig. 5. SEM micrographs of polished and plasma etched specimens prepared in the magnetic field.

equation [9],

$$\Delta E = \frac{\mu_0 \Delta \chi V H_{\text{ex}}^2}{2} \quad (5)$$

where  $\mu_0$  is the permeability in vacuum,  $\Delta \chi = \chi_{a,b} - \chi_c$  the anisotropy of the magnetic susceptibility,  $V$  the particle volume and  $H_{\text{ex}} = 10$  T. So, when  $\alpha\text{-Si}_3\text{N}_4$  is placed in a magnetic field, the crystal exhibiting magnetic susceptibility anisotropy orients itself with the direction of maximum susceptibility parallel to the field.  $c$ -Axis magnetic susceptibility of  $\text{Si}_3\text{N}_4$  being smaller than for  $a$ ,  $b$ -axis, the magnetic torque originated from a magnetic field rotates  $a$ ,  $b$ -axis of  $\alpha\text{-Si}_3\text{N}_4$  and align them parallel to the imposed magnetic field direction. During the sintering process,  $\alpha\text{-Si}_3\text{N}_4$  transforms to  $\beta\text{-Si}_3\text{N}_4$  and  $\beta\text{-Si}_3\text{N}_4$  possesses a high orientation.

Fig. 5 shows the top and side2 surfaces microstructures of the sample. In Fig. 5(a), the hexagonal-like  $\text{Si}_3\text{N}_4$  is observed on the top surface of sample, and in Fig. 5(b), the long rod-like  $\beta\text{-Si}_3\text{N}_4$  is observed on the side2 surface of the sample. The SEM photographs also confirmed X-ray results.

#### 4. Conclusions

The following results have been obtained on slip casting  $\text{Si}_3\text{N}_4$  ceramics under a high magnetic field, followed by sintering.

- (1) Preferred orientation of silicon nitride can be obtained by slip casting under a high magnetic field.

- (2) The preferred orientation degree is calculated by the  $F$  value. The silicon nitride  $a$ ,  $b$ -axis orientation is parallel to the magnetic field direction and  $c$ -axis orientation is perpendicular to the magnetic field.

#### Reference

- [1] S. Awaja, Y. Ma, W.P. Chen, H. Maeda, K. Watanabe, M. Motokawa, Magnetic field effects on synthesis process of high-Tc superconductors, *Curr. Appl. Phys.* 3 (2003) 391–395.
- [2] Q.W. Chen, Y.T. Qian, Z.Y. Chen, W.B. Wu, Z.W. Chen, G.E. Zhou, Y.H. Zhang, Hydrothermal epitaxy of highly oriented  $\text{TiO}_2$  thin-films on silicon, *Appl. Phys.* 66 (1995) 1608–1610.
- [3] K. Kakimoto, H. Kakimoto, S. Fujita, Y. Masuda, Control of crystal orientation and piezoelectric response of lead zirconate titanate thin films near the morphotropic phase boundary, *J. Am. Ceram. Soc.* 85 (2002) 1019–1021.
- [4] Y. Sakka, T.S. Suzuki, N. Tanabe, S. Asai, K. Kitazawa, Alignment of titania whisker by colloidal filtration in a high magnetic field, *Jpn. J. Appl. Phys.* 41 (2002) 1416–1418.
- [5] I.L. Marta, L. Oliveira, Kexin Chen, M.F. Jose, Ferreira, Influence of the deagglomeration procedure on aqueous dispersion, slip casting and sintering of  $\text{Si}_3\text{N}_4$ -based ceramics, *J. Eur. Ceram. Soc.* 22 (2002) 1601–1607.
- [6] R. Moreno, A. Salomoni, S. Mello Castanbo, Colloidal filtration of silicon nitride aqueous slips. Part I: Optimization of the slip parameters, *J. Eur. Ceram. Soc.* 18 (1998) 405–416.
- [7] C. Suryanarayana, M.G. Norton, *X-ray Diffraction: A Practical Approach*, Plenum Press, New York, p. 223.
- [8] Y.H. Wang, in: S.H. Xu, Z.D. Liang (Eds.), *The Fundamental of X-ray Diffraction Technology*, Atomic Energy Press, Beijing, 1993, p. 253.
- [9] Y. Sakka, T.S. Suzuki, N. Tanabe, S. Asai, K. Kitazawa, Alignment of titania whisker by colloidal filtration in a high magnetic field, *Jpn. J. Appl. Phys.* 41 (2002) 1416–1418.